Journal of Structural Geology, Vol. 14, No. 2, pp. 161 to 179, 1992
Printed in Great Britain

0191-8141/92 $05.00 + 0.00

Palaeoseismic events recorded in Archaean gold–quartz vein networks, Val d'Or, Abitibi, Quebec, Canada

ANNE-MARIE BOULLIER

Centre de Recherches Pétrographiques et Géochimiques, BP 20, 54501 Vandoeuvre-lès Nancy Cédex, France

and

FRANÇOIS ROBERT

Geological Survey of Canada, 601 Booth St., Ottawa, Canada K1A 0E8

(*Received* 7 *December* 1990; *accepted in revised form* 3 *June* 1991)

Abstract—Archaean gold–quartz vein deposits are commonly hosted in high-angle reverse shear zones and are interpreted to have formed in a regime of horizontal compression and high fluid pressure environment. This paper presents the results of a combined structural and fluid inclusion study on three gold–quartz vein deposits of the Val d'Or area (Abitibi, Quebec) consisting of subhorizontal extensional veins and E–W steeply dipping shear veins. Crack–seal structures, tourmaline fibres, stretched quartz crystals and open-space filling textures indicate that the subhorizontal veins formed by hydraulic fracturing under supralithostatic fluid pressure. CO_2-rich and H_2O + NaCl fluid inclusions, interpreted as two coexisting immiscible fluids, occur typically in microcracks of different orientations interpreted to have formed in the σ_1–σ_2 plane. Horizontal CO_2-rich fluid inclusion planes are contemporaneous with the opening of these veins (σ_3 vertical). Vertical H_2O + NaCl fluid inclusion planes, as well as some microstructures, such as deformed minerals, indicate that the same extensional veins have experienced episodic vertical shortening (σ_3 horizontal) alternating with the opening events. Deformation and slip/opening also occurred in shear veins in which preferred orientation of fluid inclusion planes is not clear, except that the H_2O + NaCl fluid inclusion planes tend to be oriented at high angles to the slip direction.

The successive opening and collapse events in subhorizontal extensional veins are correlated with deformation and slip/opening events in shear veins, respectively, and are attributed to cyclic fluid pressure fluctuations in the system. They are thus consistent with the fault-valve model: sudden drop in fluid pressure from supralithostatic to lower values induces fluid unmixing and occurs immediately post-failure following seismic rupturing along the shear zone. Sealing of the shear veins allows the fluid pressure to build up again and the subhorizontal extensional veins to form.

The intermittent change in orientation of σ_3 in horizontal extensional veins is ascribed to a total shear stress release along the neighbouring shear veins after rupture. The complex internal structures of the gold–quartz veins provide an excellent record of Archaean seismic activity along high-angle reverse faults.

INTRODUCTION

THE importance of fluids in deformation and faulting has long been recognized, as illustrated by the work of Hubbert & Rubey (1959) on the role of fluid pressure in the mechanics of overthrust faulting and by that of Secor (1965) showing the importance of high fluid pressure in the generation of extension fractures at significant depths in the crust. More recently, the interplay between fluid pressure, slip events along faults and vein development has been addressed by a number of authors (e.g. Phillips 1972, Kerrich & Allison 1978, Sibson 1981, Cox *et al.* 1986, in press, Sibson *et al.* 1988, Parry & Bruhn 1990) who pointed out that fluid pressure fluctuations are likely to accompany shear stress release during faulting, especially in the case of high-angle reverse faults. However, the details of such interplay remain poorly understood.

As recognized by Cox *et al.* (1986, in press) and Sibson *et al.* (1988), mesothermal gold–quartz vein deposits represent an ideal case for studying the role of fluids in faulting and veining, and the related fluid pressure and stress cycling. Such deposits occur predominantly in greenstone terranes and are more abundant in those of Archaean age. Typically, these veins occur in steeply dipping, reverse to reverse-oblique shear zones and have developed incrementally in regimes of horizontal compression or transpression (Sibson *et al.* 1988, Kerrich 1989, Robert 1990a). Sibson *et al.* (1988), Sibson (1989) and Cox *et al.* (in press) have proposed models in which reactivation of sealed high-angle reverse faults is triggered by fluid pressure build up and is accompanied by a fluid pressure drop related to increased fracture permeability along the fault.

In order to further understand the relation between intermittent seismic slip, gold–quartz vein development and fluid dynamics, a detailed study of textures, microstructures and fluid inclusion planes has been undertaken on gold–quartz veins of the Val d'Or district in the southeastern part of the Archaean Abitibi greenstone belt of the Superior Province in Canada (Fig. 1). The area was selected for a number of reasons: it contains typical mesothermal gold–quartz vein deposits, well exposed in several active mines, and the geometry and structural setting of the vein networks, as well as the structural evolution of the host rocks, are relatively well understood (see Robert 1990a). Finally, the presence of well developed subhorizontal extensional veins in low

strain rocks adjacent to shear zones provides a unique opportunity to unravel the details of complex variations in fluid pressure and local stress state, and to relate them to seismic activity along adjacent shear zones.

GEOLOGY OF THE DEPOSITS

Geological context

In the Val d'Or area, the Abitibi Subprovince consists of supracrustal volcanic and minor clastic sedimentary rocks, and of synvolcanic to syn- to late-kinematic intrusions of predominantly dioritic to tonalitic composition (Fig. 1). These rocks are separated from the clastic sedimentary rocks of the Pontiac Subprovince, to the south, by the Cadillac tectonic zone, described by Gunning & Ambrose (1937) and Robert (1989). Most of the volcanic and sedimentary rocks display a weak to moderate subvertical foliation, striking E–W to NW–SE, and a predominantly down-dip elongation lineation (Robert 1990a). Such a fabric geometry is recently ascribed to a N–S compression related to the Late Archaean Kenoran orogeny (Dimroth *et al.* 1983, Ludden *et al.* 1986). Greenschist grade metamorphism has affected all rock types, including late-kinematic intrusions.

In the Val d'Or district, most gold–quartz vein deposits are located within a zone up to 15 km wide on the north side of the Cadillac tectonic zone (a first-order shear zone at a district scale, Fig. 1). The deposits however, are more closely associated with neighbouring smaller scale shear zones (second- and third-order shear zones, Robert 1990a). Gold–quartz veins and their host structures formed late in the geological evolution of the Val d'Or district. They cross-cut all rock types including late-kinematic intrusions, and were emplaced after the peak of the greenschist metamorphism. Therefore these deposits represent one of the last geological events in the Val d'Or area and are not overprinted by any significant metamorphism or deformation (Robert 1990b). This late timing of gold mineralization is supported by recent geochronological data (Wong *et al.* 1989, Zweng & Mortensen 1989, Jemielta *et al.* 1990).

Geology and structure of the deposits

Most mineralized zones consist of gold–quartz veins and their adjacent altered wall-rocks. The deposits themselves are networks of various types of veins (filled fractures) hosted by, or associated with, second- and third-order (brittle–ductile) shear zones (Robert & Brown 1986a, Robert 1990b). Following the classification of Sibson (1990), two main types of veins are distinguished on the basis of their internal structure and the orientation of opening vectors relative to the vein walls: shear veins and extensional veins (opening vector nearly parallel and nearly perpendicular to the vein walls, respectively). Individual deposits consist of different combinations of these types of veins.

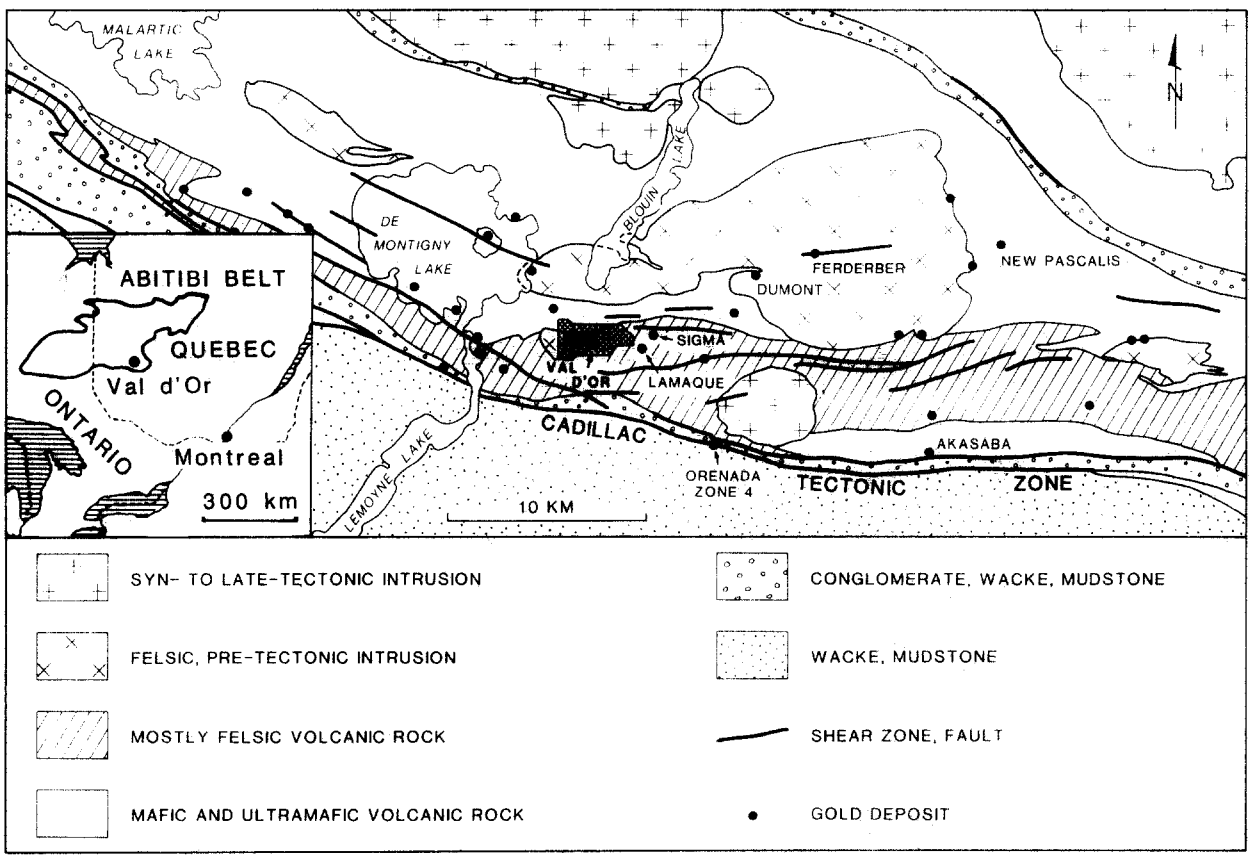

Fig. 1. Simplified map of the Val d'Or area showing distribution of gold deposits (after Robert 1990b). Inset shows Abitibi belt and location of Val d'Or area.

The veins are mainly composed of quartz and tourmaline, with subordinate amounts of carbonate minerals, chlorite, pyrite, pyrrhotite, scheelite and free-gold. They are surrounded by zoned alteration envelopes dominated by carbonatization of the wall rocks (Robert & Brown 1986b). Studies of fluid inclusions (Robert & Kelly 1987) and of hydrothermal alteration envelopes (Robert & Brown 1986b, Guha *et al.* 1991) indicate that, in general, the mineralizing fluid was mainly a low salinity, CO_2-bearing fluid with variable amounts of CH_4.

Fluid inclusion studies and oxygen isotope analyses of wall-rock alteration provide consistent estimates of temperature during vein formation (270–450°C, Kerrich 1986; 300–400°C, Robert & Kelly 1987). Depths of vein formation are not well constrained but are probably in the range of 7–14 km (2–4 kbar, Brown & Lamb 1986, Kerrich 1986, Robert & Kelly 1987). Therefore, they formed at a structural level corresponding approximately with the brittle–ductile transition zone in the continental crust (Robert & Brown 1986a) or with the base of seismogenic zone (Sibson *et al.* 1988).

Samples from three mines have been studied in detail: the Sigma, New Pascalis and Dumont-Bras d'Or mines (Fig. 1). The Sigma deposit is hosted in metavolcanic rocks, intruded by two generations of pre-ore diorite intrusions, and has been described by Robert & Brown (1986a,b). It consists of shear veins in E–W-striking, steeply S-dipping, reverse shear zones and in a poorly developed N-dipping conjugate set, and of subhorizontal extensional veins developed preferentially in the most competent host rock between the ductile shear zones (Fig. 2).

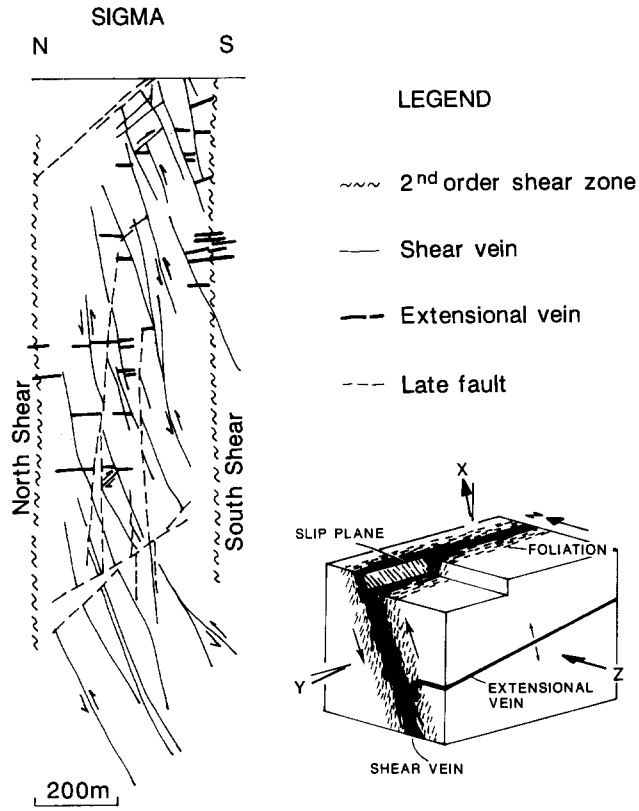

Fig. 2. Cross-section through the Sigma Mine (after Robert & Brown 1986a). The extensional veins and shear veins are localized between two second-order shear zones. Block diagram illustrates general relationships among extensional veins, shear veins and structural elements, from which bulk strain axes are deduced (after Poulsen & Robert 1989).

At the New Pascalis (L.C. Beliveau) Mine (Fig. 1), mineralized veins are confined to N–S-striking, subvertical diorite dykes intruding volcanic agglomerates (Gaumond 1986). The vein network consists of subhorizontal extensional veins (5%), of shear veins in vertical or moderately S-dipping E–W shear zones and their associated 'en échelon' extensional veins, both of which collectively represent 80% of the veins. Figure 3 shows the down-dip termination of a moderately dipping shear vein, en échelon veins indicating reverse movements, and a horizontal extensional vein. Small E–W vertical extensional veins are also common at the New Pascalis Mine.

At the Dumont-Bras d'Or Mine (Fig. 1), the mineralized veins are contained in a single E–W reverse shear zone dipping 70°S; subhorizontal extensional veins are rare. It is similar to the Ferderber gold deposit located in the centre of the Bourlamaque batholith and described by Vu (1990).

Despite differences in the nature and complexity of the vein networks, the three deposits, as well as many others in the area (Robert 1990a), combine one or more sets of E–W, moderately to steeply dipping reverse shear zones with variably developed subhorizontal extensional veins. Conflicting cross-cutting relationships between the different types of veins indicate that they are broadly contemporaneous and cogenetic. In most cases, it is possible to reconstruct the bulk strain axes of the vein networks (Poulsen & Robert 1989, Robert 1990a), which record approximately N–S horizontal shortening and subvertical elongation, ascribed to a late N–S compression, as illustrated in Fig. 2. Finite displacement along individual shear zones, as estimated from integrated strain analyses (Ramsay & Graham 1970) and offset of markers, falls in the range of a few metres to a few tens of metres (see Robert 1990a). It should be noted, however, that macroscopic evidence for local normal faulting has also been reported by previous authors at the Sigma (Robert *et al.* 1983) and the Pascalis Nord deposits (Tessier 1990).

Characteristics of the veins

Exensional veins are best developed at the Sigma Mine. They have dips of less than 30° and are characterized by regular planar walls. They range in thickness from a few centimetres up to 1 m, and extend away from shear veins in low strain rocks for distances up to several tens of metres (Robert & Brown 1986a, Robert 1990a). Extensional veins consist of one or more major growth layers, corresponding to major individual opening increments. These have sharp, well-defined boundaries, and contain several types of internal mesostructures such as inclusion bands and trails, mineral fibres, and euhedral

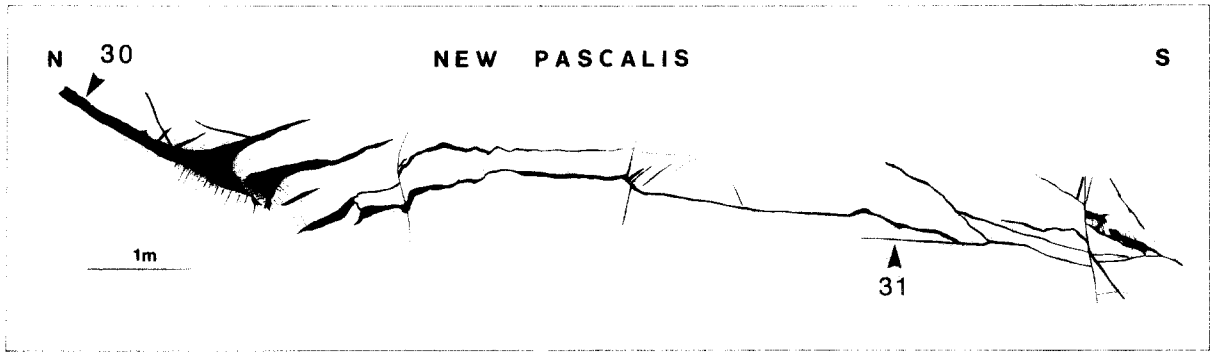

Fig. 3. Vertical cross-section view of a moderately dipping shear vein from the New Pascalis Mine. Note foliation on footwall of the vein, and extensional veins on its hanging wall, indicating a reverse sense of shear. 30 and 31 are locations of samples 89RAO30 and 89RAO31, respectively.

scheelite and carbonate crystals (Fig. 4b). Individual major growth layers can be traced laterally over a few metres. The opening vector, defined by offset of markers or by the tourmaline fibres, is typically vertical (Figs. 4a–c), despite small variations in the dip of the extensional veins. Slight variations of the opening direction are locally observed from one major growth layer to another (Fig. 4c; see below).

Shear veins are steeply to moderately dipping and localized in the central portion of shear zones. They are not as extensive as the host shear zone and several shear veins may occur along the same shear zone. Shear veins range in thickness from several centimetres up to a few metres and reach several tens of metres in their longest dimension. The reverse nature of the host shear zone can be deduced from the sigmoidal pattern of foliation, dragfolding of small deformed extensional veins (Fig. 5a) and subvertical lineation in the shear zone. Shear veins are typically banded and consist of tourmaline layers and altered wall-rock slivers separating quartz–carbonate lenses, and are interpreted as the result of a complex sequence of opening, slip, deformation and amalgamation of smaller veins (Robert & Brown 1986a). Some shearing or slip is localized on these tourmaline layers as indicated by down-dip striations and tourmaline slickenfibres. In several cases, such slip can be shown to be reverse and to accompany and control, rather than post-date, vein growth (see Robert 1990a). Severe buckling and folding of small subhorizontal extensional veins (fig. 6 in Robert & Brown 1986a) (Fig. 5a) indicate that significant shortening occurred across the shear zone. The presence of small horizontal veins and boudinage of the shear veins (Fig. 5b) also indicates vertical extension of the shear veins, which is consistent with the down-dip elongation lineation on the foliation plane.

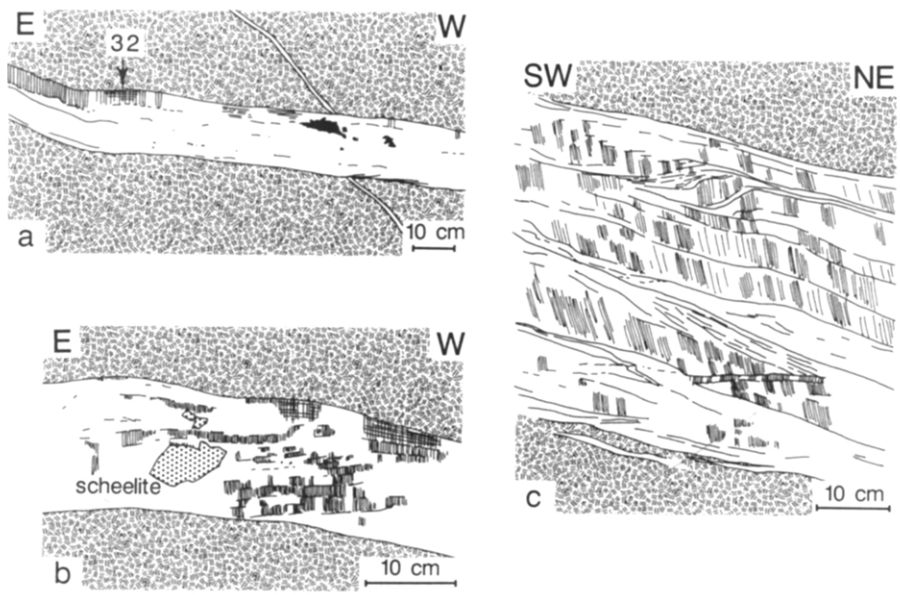

Fig. 4. Mesoscopic characteristics of subhorizontal extensional veins as seen on vertical stope walls in the Sigma Mine. (a) Vertical tourmaline fibres indicate a subvertical opening vector which is consistent with the offset of small steeper vein. Location of sample 89RAO32 is shown as 32. (b) Euhedral scheelite crystal suggesting open-space filling in part of the vein; crack–seal inclusion bands are shown by thin lines parallel to vein walls. (c) Multistage extensional vein showing a complex history. Subvertical lines indicate orientation of tourmaline fibres. Lines subparallel to the walls separate different growth layers or major opening events.

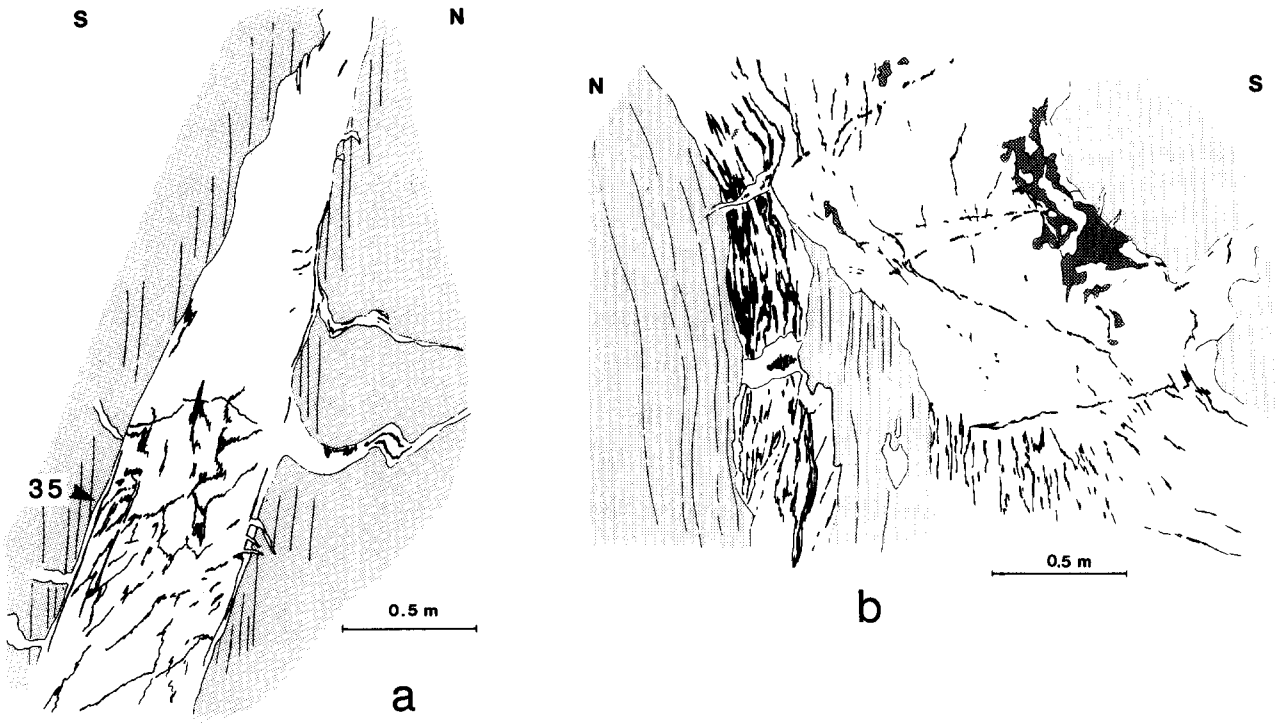

Fig. 5. Mesoscopic characteristics of shear veins, as observed on vertical stope walls. (a) Shear vein at Sigma Mine; relationship between schistosity in foliated wall rock and the vein itself indicates a reverse sense of shear. Note small folded extensional veins on both sides of shear vein. Location of sample 89RAO35 is shown as 35. Black lines are tourmaline. (b) Shear vein at Dumont-Bras d'Or Mine. Pyrite is medium grey, black lines are tourmaline. Note boudinage of small vertical vein and ribbon structure of both veins. (a) & (b) show shallowly dipping tourmaline layers which may be interpreted as extensional veins related to stretching of the shear veins.

INTERNAL STRUCTURE OF THE VEINS

In this study, emphasis has been placed on the internal structures and microstructures of the gold–quartz veins, as they preserve an excellent record of the complex history of incremental vein development. A variety of structures are observed in both extensional and fault veins. These structures are grouped into two categories: those representing vein growth and material addition, and those representing deformation of existing vein material. As the degree of development and preservation of these structures differ in the two vein types, they are described separately for each.

Subhorizontal extensional veins—structures related to vein growth

Four main types of growth structures are observed within individual major growth layers (see Fig. 6a): crack–seal structures, mineral fibres, stretched quartz crystals and open-space filling textures.

Crack–seal structures analogous to those previously described by Ramsay (1980) and Cox & Etheridge (1983) are relatively common in the extensional veins. They are defined by very regular lines of small crystals of albite, calcite, rutile, chlorite and tourmaline, similar to those of the vein walls. The lines (or inclusion bands) are parallel to each other and reproduce the commonly delicate geometry of the wall (Fig. 6b). Spacing between the inclusion bands is regular, but seems to depend on the grain size of the wall rock. For example, spacing is 25 μm on average for crack–seal increments formed adjacent to layers of very fine tourmaline (<10 μm), and is of the order of 200 μm for crack–seal increments formed adjacent to volcanic rocks in which plagioclase phenocrysts are 100–200 μm in diameter. Inclusion bands locally make up the whole thickness of a major growth layer, i.e. they are repeated over a cumulative thickness in excess of 2.5 cm (about 1000 lines) without any disturbance. They have been observed to extend laterally on a metre scale in the stopes. In some areas, inclusion bands terminate laterally for a few increments leaving some spaces in which rosettes of small tourmaline needles developed. Inclusion bands are also commonly interrupted along quartz grain boundaries, and therefore, define columnar inclusion band-rich crystals separated by clear quartz crystals with the same crystallographic orientation. These structures are similar to those described by Henderson *et al.* (1990). Inclusion trails (Ramsay 1980) are almost ubiquitous and show slight variations (up to 30°) in their orientation relative to the vein walls.

Mineral fibres are relatively common in subhorizontal extensional veins, and are generally perpendicular, or at a high angle, to the vein walls. Tourmaline fibres (Fig. 6a) are the most abundant, but fibres of quartz and carbonate are also present. Two types of monocrystalline tourmaline fibres can be distinguished depending on their size. Large fibres (>1 μm, Fig. 6c) are well crystallized. Their *c*-axes are generally parallel, but are locally

oblique (up to 42°) to the elongation of the fibres. They contain large (up to 0.1 mm thick) cracks that are most commonly oriented at high angles to the *c*-axis of the fibre; where healed by new tourmaline, these cracks are outlined by differences in colour and by tubular primary fluid inclusions along the *c*-axis (Fig. 6d). The cracks do not extend into neighbouring quartz crystals. Hair-like tourmaline fibres ($\ll 1\,\mu$m in diameter, Fig. 7a) are included in quartz or constitute fibrous skeins.

Stretched quartz crystals, similar to those described by Cox & Etheridge (1983) and Ramsay & Huber (1983), have also been observed in extensional veins. They are long and narrow (0.5 to a few mm) crystals with *c*-axes at high angles to the walls and show irregular grain boundaries.

Open-space filling textures are common in extensional veins. Rosettes of tourmaline or coarse euhedral crystals of other vein minerals (calcite, muscovite, scheelite) are attached to the vein walls, which indicate crystallization in a fluid-filled cavity (see Fig. 4b). Such textures have been described in detail by Robert & Brown (1986b). Some very large and clear quartz crystals exhibit Brazil twins and primary fluid inclusions along pyramidal planes. Such twins, described in euhedral crystals (Frondel 1962), are growth twins and indicate crystallization in open-spaces. In some cases, the minimum thickness of individual openings is up to 8 cm, as indicated by the dimensions of the largest tourmaline rosettes and scheelite crystals.

The four types of textures described above may coexist in a single vein, and moreover, in a single growth layer. Rosettes of tourmaline are locally observed to form adjacent to tourmaline fibres or stretched quartz crystals, and crack–seal lines are seen to laterally terminate against tourmaline fibres. The significance and cause of these lateral variations in vein textures, from open-space filling to crack–seal to fibres and stretched crystals is not understood at present.

The opening vector of the extensional veins can be determined from the inclusion trails in the minerals with crack–seal structures (Ramsay 1980, Cox & Etheridge 1983, Cox 1987) and from displacement of external markers. These criteria are in general more reliable than the orientation of the fibres which are often determined by the orientation of the vein walls (Cox 1987). However, in several cases tourmaline fibres are parallel to inclusion trails in crack–seal structures and, therefore, tourmaline fibres have also been used. Despite the fact that most extensional veins formed by multiple growth events, there is generally a good correspondence between the finite opening direction of the vein, indicated by the displacement of external markers, and the various increments of opening, indicated by inclusion trails and mineral fibres (Fig. 4a). In a number of cases, however, individual increments record a slightly different opening direction. Figure 4 gives examples of extensional veins showing simple and complex opening histories.

On the basis of the geometry of the veins and of the orientation of the opening vector, subhorizontal extensional veins are attributed to overall vertical extensional-shear fracturing, mostly indicated by layers of very fine tourmaline fibres.

Extensional veins—deformation structures

Several structures indicate that the subhorizontal extensional veins have undergone some degree of deformation. For example, quartz crystals exhibit varying amounts of plastic deformation and grain-boundary recrystallization. Subgrain boundaries are prismatic and are either at high angles or nearly parallel to the vein walls, depending on the orientation of the host quartz crystal. Deformation lamellae have also been observed locally. Different increments of opening in a single vein commonly display contrasting degrees of plastic deformation, and clear undeformed quartz may coexist with deformed and recrystallized quartz (Fig. 6c). The less deformed crystals (no undulatory extinction, no subgrains) are observed either where quartz is associated with tourmaline fibres, or within the youngest growth layers (Fig. 6c).

In some samples, massive tourmaline layers display small vertical quartz-filled fractures corresponding to about 5% stretching in the horizontal direction (Fig. 8a). Individual horizontal tourmaline crystals locally show up to 11% horizontal stretching. Small vertical quartz veins (0.2 mm) cross-cutting hair-like tourmaline fibres correspond also to a vertical shortening, which is also indicated by incipient folding or faulting of vertical tourmaline fibres (Figs. 7a and 8b & c).

Finally, numerous healed microcracks defined by fluid inclusion planes cut across the quartz and tourmaline crystals (Fig. 7b) and represent brittle deformation of the veins; these are discussed in more detail below. The abundance of fluid inclusion planes is much higher in the oldest increment of opening than in the youngest (Fig. 7c), suggesting that they were formed continuously throughout the formation of the vein. This is further supported by the presence of a fragment of deformed fluid-inclusion-rich quartz entirely enclosed in a younger, undeformed clear quartz as shown in Fig. 7(d).

Shear veins—structures related to vein growth

The primary growth structures observed in extensional veins are not as common in shear veins. Because of the generally higher degree of deformation in shear veins, it is not clear if the relative scarcity of primary growth structures is related to their low degree of preservation or if it reflects fundamental differences in vein opening and growth processes. Local euhedral crystals of scheelite and pyrite attached to the vein walls, as well as tourmaline rosettes (Fig. 9a) and a few clear quartz crystals showing Brazil twins indicate, at least locally, open-space filling. Crack–seal structures (Fig. 9a) are also locally preserved and do not differ significantly from those in subhorizontal extensional veins except for their limited extension (less than 50 increments). Hair-like tourmaline needles are often observed and are subvertical, whereas large tourmaline fibres are absent.

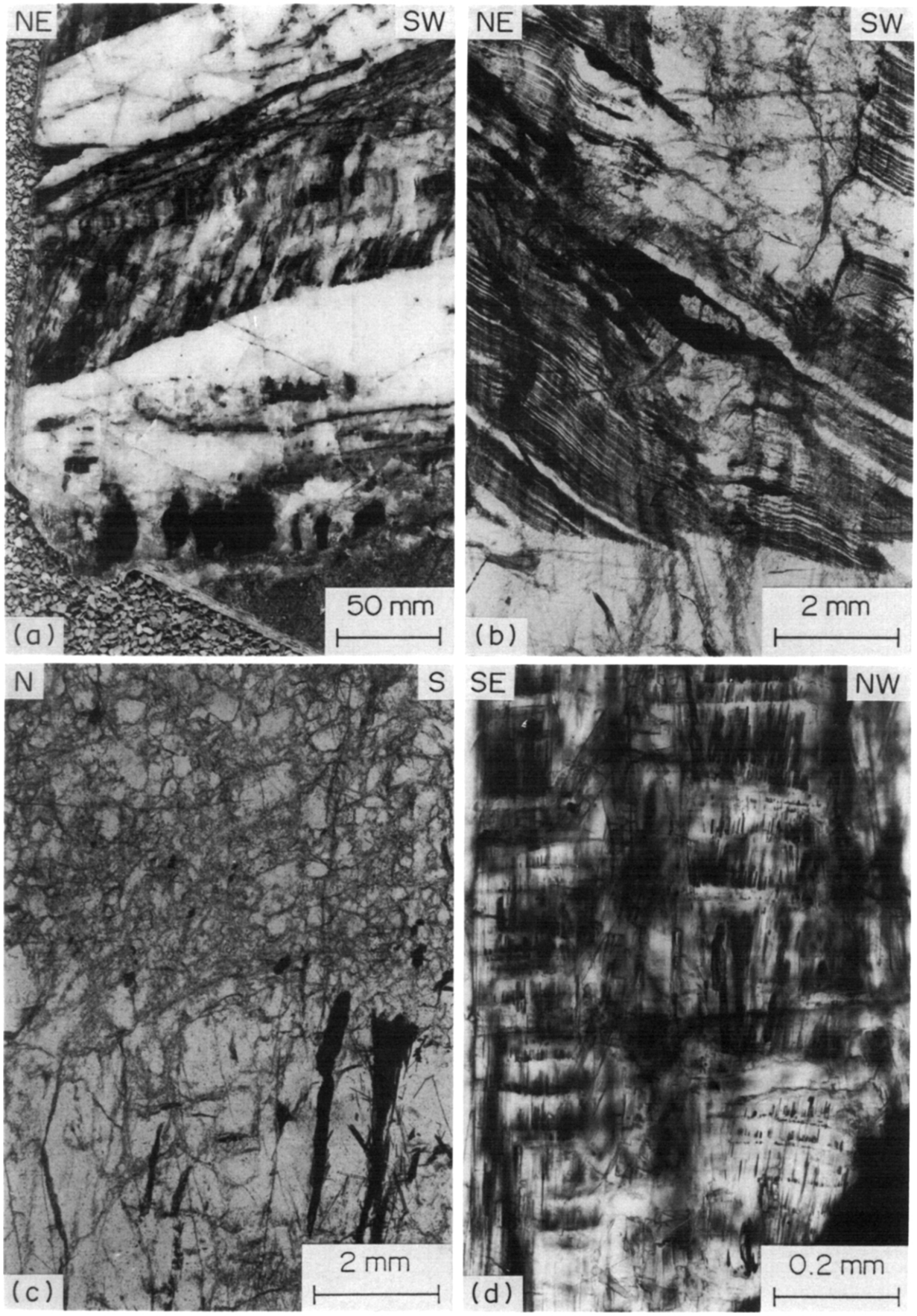

Fig. 6. Photomicrographs in plane light of vertical sections in subhorizontal extensional veins. (a) Polished section from same vein as in Fig. 4(c), showing tourmaline fibres and tourmaline layers outlining different growth layers. (b) Crack–seal structures within a growth layer in a thick section; note regularity of crack–seal lines which are cross-cut by a younger growth layer (bottom) and the interruption of crack–seal lines (centre). (c) Juxtaposition of two growth layers; the older is outlined by deformed, inclusion-rich quartz crystals and the younger is made up of clear quartz with a few fluid inclusion planes and millimetric tourmaline fibres (black). (d) Large tourmaline fibre displaying horizontal cracks outlined by tubular fluid inclusions.

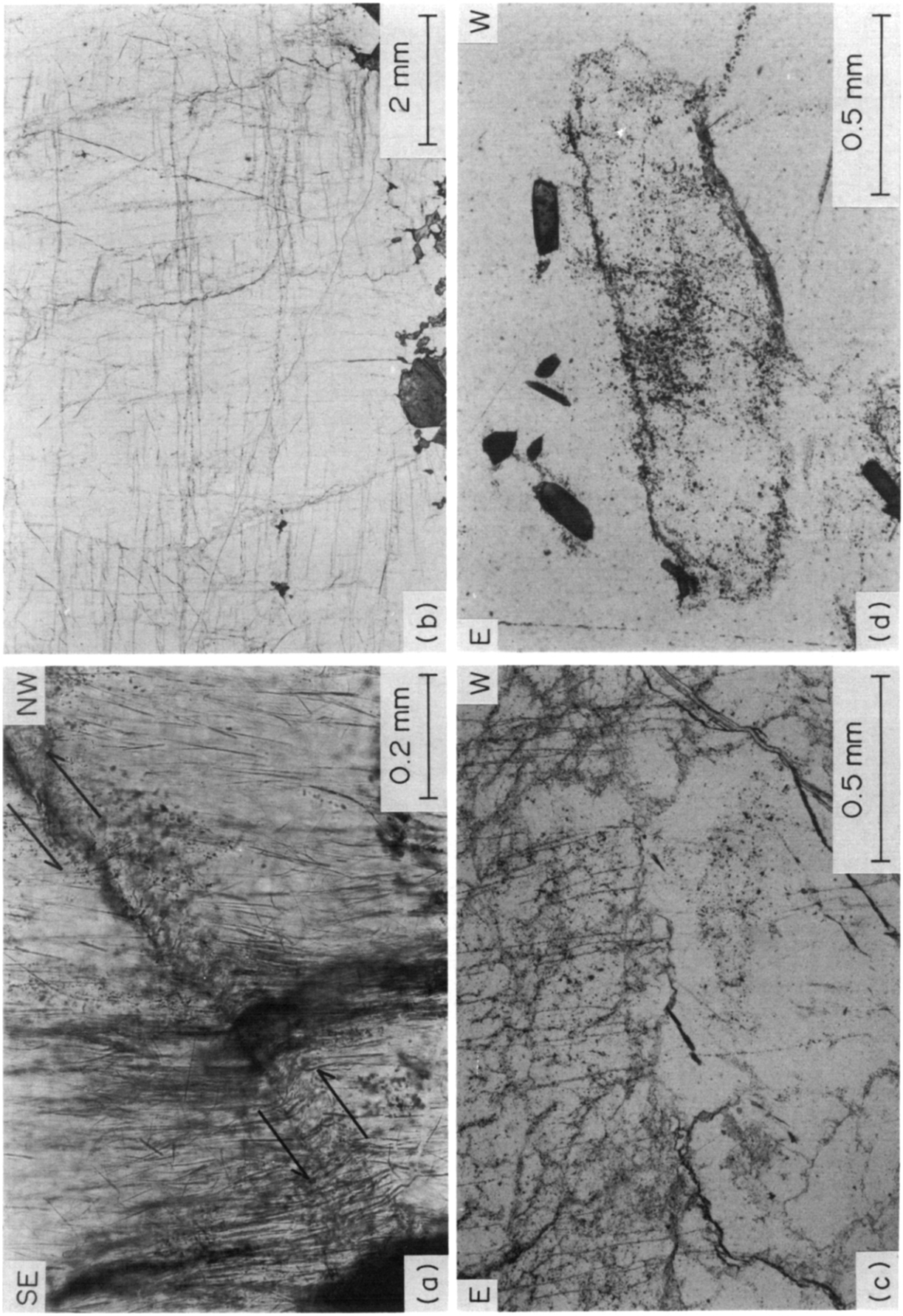

Fig. 7. (a) Kink of fine tourmaline fibres at a grain boundary, indicating vertical shortening. (b) Fluid inclusion planes showing two main orientations: one parallel and the other perpendicular to vein walls. (c) Juxtaposition of two increments of opening, the oldest (top) showing higher abundance of fluid inclusion planes than the youngest, clear increment (bottom), suggesting that these fluid inclusion planes were formed continuously throughout formation of the vein. (d) Xenolith of an older, deformed, and inclusion-rich quartz grain incorporated into younger, clear, undeformed quartz. (a)–(d) in plane light.

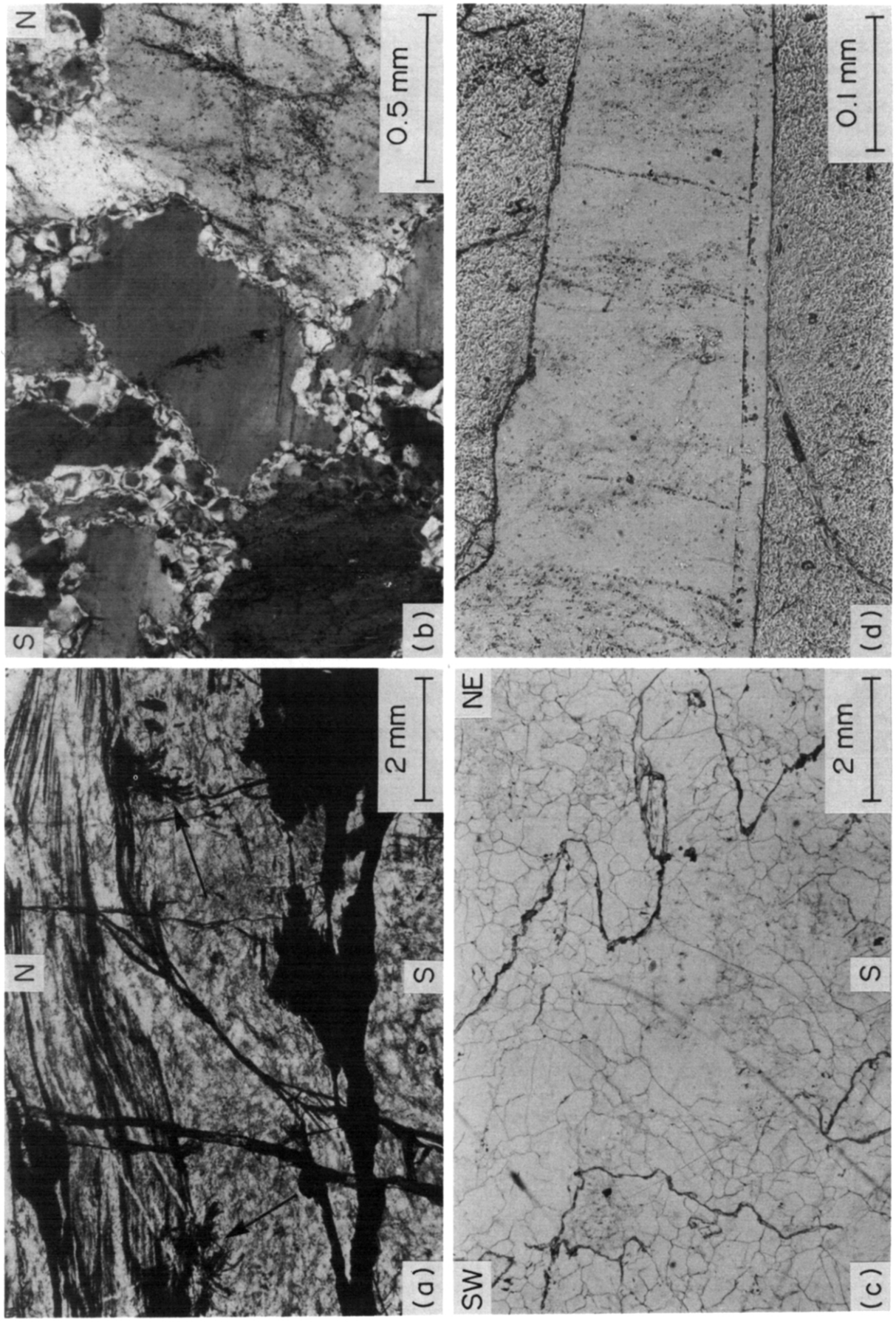

Fig. 9. Photomicrographs of shear veins. (a) Horizontal thick section of a shear vein (sample 89RAO35) showing crack–seal textures and deformed tourmaline rosettes (arrows). (b) Deformed fluid inclusion-rich quartz grain coexisting with smaller grains, due to dynamic recrystallization, and with larger less deformed inclusion-free quartz grains; crossed nicols. (c) Stylolites in a vertical thin section of a shear vein, Dumont-Bras d'Or Mine. (d) Scheelite crystal displaying quartz-filled microcrack in which secondary fluid inclusion planes are truncated by a crack–seal increment. (a), (c) & (d) in plane light.

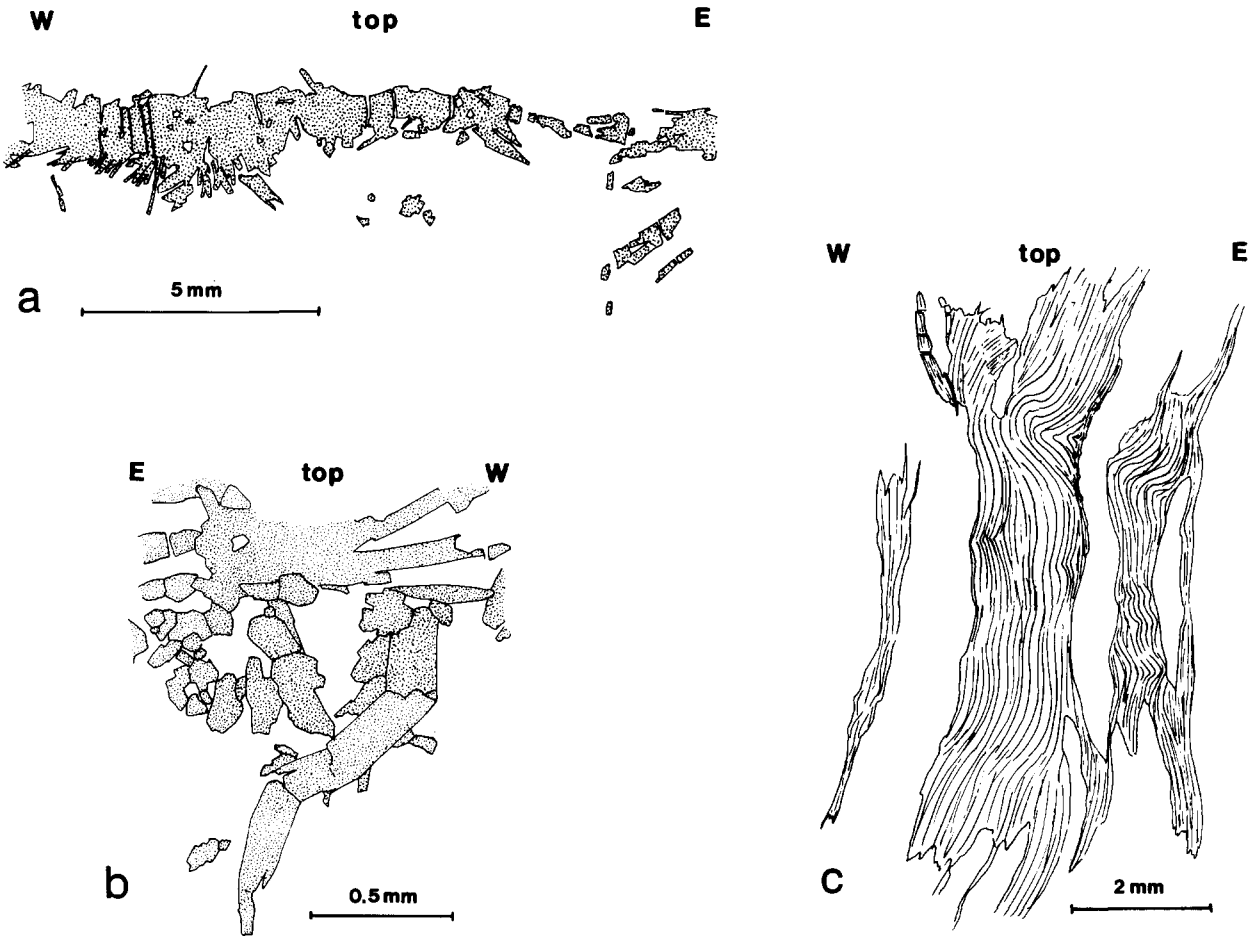

Fig. 8. Deformation structures in subhorizontal extensional veins; drawings after photomicrographs of vertical sections. (a) Boudinage (5%) of a horizontal tourmaline layer. (b) Kinked tourmaline crystal. (c) Folded hairy tourmaline fibres.

Shear veins—deformation structures

The internal structure of the shear veins is dominated by deformation features. Plastic deformation occurred in quartz crystals as shown by the presence of prismatic subgrain boundaries, undulatory extinction and subgrains (grain-size 30–50 μm on average). Recrystallization took place at grain boundaries and gave way to less deformed, fluid inclusion-free crystals. Recrystallized grains are 50–400 μm in diameter (Fig. 9b). The intensity of plastic deformation varies from one growth layer to another in a single vein, as shown by large, almost undeformed quartz crystals coexisting with crystals exhibiting undulatory extinction or intense polygonization. Stylolites are common in shear veins and are outlined by white mica, tourmaline and chlorite (Fig. 9c). The stylolitic peaks are mainly N–S and horizontal and are therefore consistent with a horizontal N–S compression.

Although mesoscopic textures indicate overall reverse movement along the shear veins, some microscopic textures indicate that small amounts of normal displacement or extensional shearing occurred locally on tourmaline slip planes. Figure 10 illustrates such a case in the New Pascalis Mine, where a small calcite veinlet is sheared along shear planes parallel to tourmaline layers.

As in subhorizontal extensional veins, fluid inclusion planes are numerous in shear veins and indicate intensive microfracturing. These planes show variable degrees of reworking by plastic deformation.

FLUID INCLUSION PLANES

Fluid inclusion planes represent closed and healed microcracks in which a fluid has been trapped and has enhanced the healing of the host crystal. By analogy with experimental results (Brace & Bombolakis 1963, Tapponnier & Brace 1976, Krantz 1979), they are interpreted as mode I microcracks, i.e. tensile cracks in the σ_1–σ_2 plane perpendicular to the least principal compressive stress σ_3. This interpretation is suggested by the lack of strain or lateral displacement in the host crystal, at least for the greatest majority of observed natural

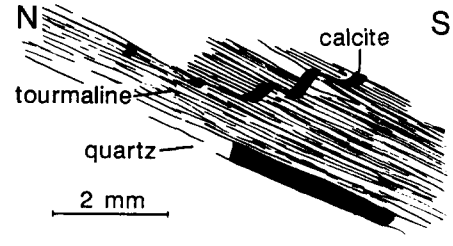

Fig. 10. Drawing after a photomicrograph of a shear vein (89RAO30), showing a calcite veinlet that has been sheared with normal shear sense.

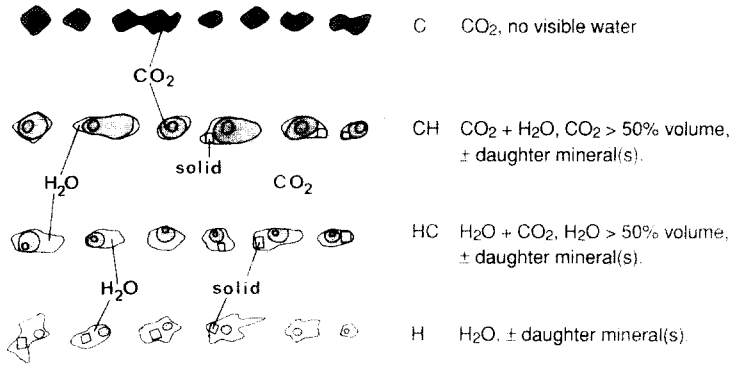

Fig. 11. Different types of fluid inclusions as defined optically for classification of fluid inclusion planes during measurement of their preferred orientation.

microcracks in rocks (see Krantz 1983). It is also supported by the lack of offset of grain boundaries or of other intersected healed microcracks in the studied samples. The experiments of Smith & Evans (1984) and Brantley *et al.* (1990) show that healing of microcracks in the presence of fluids is thermally activated, depends on the width of the crack, and may occur in as little as 1–2 days at elevated temperatures.

The preferred orientation of fluid inclusion planes has been used by several authors to reconstruct the stress state in metamorphic, granitic or sedimentary environments (Tuttle 1949, Wise 1964, Lespinasse & Pêcher 1986, Laubach 1989, Ploegsma 1989, Ren *et al.* 1989). In the present study, fluid inclusion planes are used as markers of the stress state during the history of the veins and as markers of the fluid pathways. A study of preferred orientation of the fluid inclusion planes was performed, recording the nature of the fluid and the relative importance of the plane (size of the inclusions, length of the plane).

On the basis of petrographic observations, four main types of fluid inclusions have been distinguished (Fig. 11): C (carbonic), CH ($CO_2 > H_2O$, ±NaCl), HC ($H_2O > CO_2$, ±NaCl) and H (H_2O, ±NaCl). These types compare very well with those described by Robert & Kelly (1987). In the absence of accompanying thermometric measurements, and considering the small size of the inclusions (generally less than 5 μm), some uncertainties are inherent in this classification and some inclusions are probably assigned to the wrong type. Moreover, a complete spectrum of composition is observed between types C and H inclusions and CH and HC in fact represent intermediate compositions.

The orientation of fluid inclusion planes has been determined on oriented, doubly polished thick (200 μm) sections used for conventional fluid inclusion studies. Both the azimuths and the projected widths of the planes were measured on a standard petrographic microscope with a calibrated micrometer. Using the calibrated micrometric focusing screw to determine the thickness of the plate, it was possible to convert the projected width of the fluid inclusion plane into its dip. With each sample, care was taken to make measurements on sections oriented such that a large number of fluid inclusion planes were at high to moderate angles to the section, in order to obtain better precision. However, unlike the universal stage, this method allows measurements of planes with very low dips in a thick section.

The orientation of fluid inclusion planes was studied in detail in two pairs of shear veins and associated extensional veins from the Sigma and New Pascalis mines.

Orientation of the fluid inclusion planes in subhorizontal extensional veins

Sample 89RAO32 comes from a subhorizontal, 15 cm-thick extensional vein in the Sigma Mine that shows four main stages of opening (see Fig. 4a). The orientation of fluid inclusion planes was measured for three of these opening stages. However, as there are no differences in orientation from one stage to another, the data are presented together (Fig. 12a).

It is clear that the CO_2-rich (type C) fluid inclusion planes are mostly subhorizontal, i.e. nearly parallel to the vein walls (Fig. 12a). This is also true for a large number of the CO_2–H_2O (type CH) fluid inclusion planes. Conversely, the aqueous fluid (type H) inclusion planes are subvertical, i.e. nearly perpendicular to the vein walls, with dominant strikes at 100–110° and 0–020°. CH and HC types of fluid inclusion planes which are intermediate in composition, are actually intermediate in orientation between the two end-members C and H types.

In this sample, fluid inclusion planes display reworking by very small vertical cracks similar to those described by Roedder (1984, p. 69). Measurement of the orientations of these microcracks, easily observed in a N–S vertical section (Fig. 13), demonstrates that they are not crystallographically controlled but are mainly E–W and vertical.

Sample 89RAO31 comes from the small subhorizontal extensional vein (4 cm thick) from the New Pascalis Mine, shown in Fig. 3. The orientations of the fluid inclusion planes (Fig. 14a) are similar to those in the extensional vein from Sigma Mine, with the same partitioning of C and H types in horizontal and vertical microcracks, respectively. The only difference is that the aqueous planes at New Pascalis do not show any N–S vertical orientation.

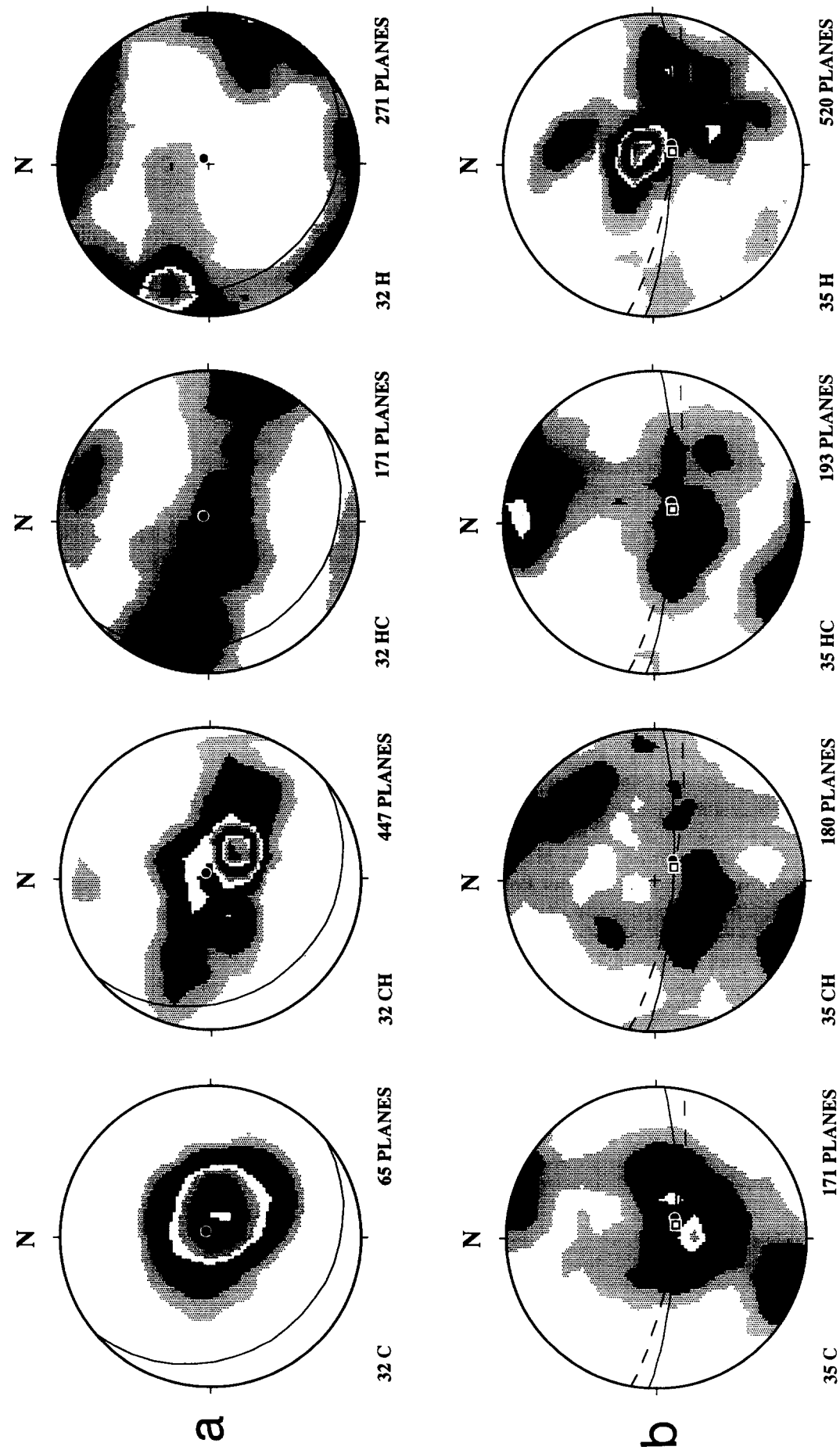

Fig. 12. Equal-area, lower-hemisphere stereographic projections of fluid inclusion planes in two samples from the Sigma Mine. Kamb contours. Orientation data were treated with 'STEREONET' software (R. W. Allmendinger, Cornell University, Ithaca). (a) Subhorizontal extensional vein, sample 89RAO32. Plane of vein indicated by great circle and tourmaline fibres by large filled dot (vertical). (b) Shear vein, sample 89RAO35. Plane of vein indicated by continuous great circle, slip plane by discontinuous great circle, tourmaline lineation on schistosity by large filled dot, and tourmaline slickenlines on slip plane by large open square.

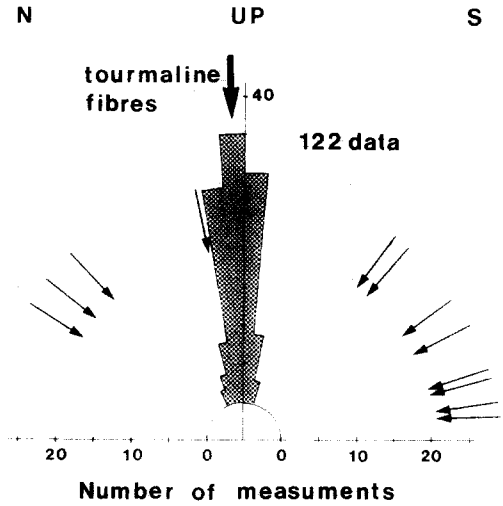

Fig. 13. Rose diagram showing orientation of microcracks originating on fluid inclusion planes in a vertical N–S thick section of extensional vein 89RAO32. Arrows indicate projected trace orientation of the *c*-axis of the measured quartz grains.

Orientation of fluid inclusion planes in shear veins

Sample 89RAO35 is from a 45 cm-wide vein within a reverse E–W shear zone containing tourmaline slip planes (Fig. 5a) from the Sigma Mine. Tourmaline lineations on the foliation and tourmaline striations on the slip planes are both down-dip. Measurements were performed on different layers of quartz contained in two perpendicular sections (one subhorizontal and one vertical N–S). Except for variations in the number of planes and the degree of reworking of the fluid inclusion planes, all the layers show similar patterns of orientation and consequently are presented together (Fig. 12b). The orientation patterns of fluid inclusion planes are not as clear as for the subhorizontal extensional veins. Poles of CO_2-rich planes (type C) define a girdle at a high angle to the vein walls with a maximum parallel to the slip direction (Fig. 12b); i.e. they vary in dip from horizontal to N- and S-dipping. Fluid inclusion planes of CH and HC types define a similar pattern, except that poles of HC planes indicate that these planes are dominantly E–W and vertical. The planes of H type inclusions display a more complex orientation, but most of the planes are at a high angle to the vein walls and strong concentrations of poles lie near the slip direction along the shear zone.

Sample 89RAO30 was collected from a shallowly dipping, E–W-striking reverse shear zone (Fig. 3) with small-scale evidence for normal faulting (Fig. 10) from the New Pascalis Mine. In this case, the walls of the vein also acted as slip planes, and contain down-dip tourmaline striations. The CO_2 planes (type C) are at a high angle to the vein walls and display an average NE dip (Fig. 14b). Again the aqueous planes (type H) are oriented nearly perpendicular to the vein walls and to the slip direction.

One important point emerging from this study is that the orientation of fluid inclusion planes within the veins is not random and depends strongly on the type and orientation of the veins. The presence of both horizontal and vertical healed microcracks within the extensional veins records both vertical extension and vertical shortening of the veins, consistent with microstructural observations. In both vein types studied, there is also a strong partitioning of end-member fluids in different sets of healed microfractures; the CO_2-rich fluids occur in horizontal microfractures and the aqueous fluids occur dominantly in vertical microfractures. In shear veins, the trends are not so clear but aqueous fluid inclusion planes tend to be oriented at high angles to the slip direction along the shear vein.

INTERPRETATIONS

Relative timing of incremental vein growth and deformation

In both types of veins, evidence has been found from internal structures and fluid inclusion planes for *alternating* episodes of vein growth and deformation, rather than for deformation completely post-dating vein growth as inferred by Robert & Kelly (1987). The character and history of deformation in both types of veins is discussed below.

Deformation structures indicate that the subhorizontal extensional veins underwent two main types of deformation: vertical extension (growth of tourmaline fibres, opening of horizontal fluid inclusion planes), which may be related to repeated extensional opening of the vein, and vertical shortening (folding of the tourmaline fibres, boudinage of tourmaline layers, opening of subvertical fluid inclusion planes), which seems incompatible with the formation of these veins. Several observations indicate, however, that the vertical shortening took place intermittently during the growth history of the vein rather than during a later tectonic event. They include different degrees of plastic deformation for different increments of opening (Fig. 6c), and higher density of fluid inclusion planes in older increments than in younger (Figs. 7c & d). Thus, the incremental development of the extensional veins comprises alternating episodes of vertical extension and vertical shortening.

In the shear veins, highly deformed quartz grains containing deformed fluid inclusion planes have recrystallized into inclusion-free quartz grains which again are slightly deformed and cross-cut by fluid inclusion planes. Figure 9(b) shows an example of such a juxtaposition of variably deformed quartz grains, and Fig. 9(d) shows a scheelite crystal cut by a quartz veinlet in which a crack–seal increment truncates fluid inclusion planes. Microfracturing thus occurred intermittently during the whole history of the shear veins, which comprises alternating episodes of opening, crystallization, plastic and brittle deformation, as proposed by Robert & Brown (1986a). The strain conditions responsible for shear vein deformation cannot be as easily interpreted as for extensional veins because plastic deformation has perturbed the fluid inclusion planes. However, it may be noted that most fluid inclusion planes are oriented at high angles to

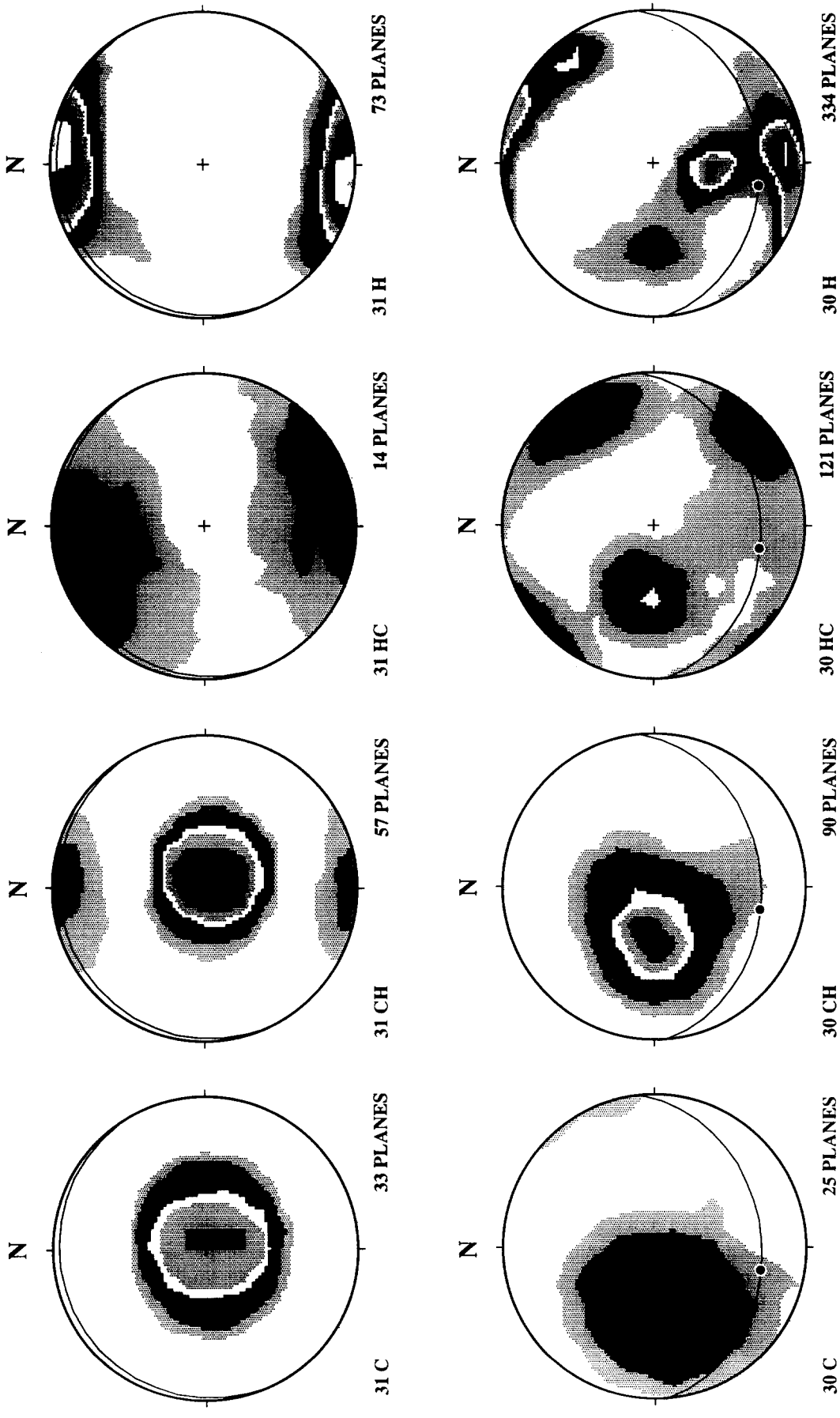

Fig. 14. Equal-area, lower-hemisphere stereographic projections of fluid inclusion planes in two samples from the New Pascalis Mine. Kamb contours (2 sigma contour interval). (a) Subhorizontal extensional vein, sample 89RAO31. Plane of vein indicated by great circle. (b) Shear vein, sample 89RAO30. Plane of vein indicated by continuous great circle, and tourmaline slickenlines on vein wall by large filled dot.

the movement direction, which is consistent with extension along that direction. In addition, the N–S horizontal stylolitic peaks indicate that the veins also underwent some N–S horizontal shortening.

The microstructural and fluid inclusion evidence presented above suggest that reversals in shortening direction occurred during the development of extensional veins and that cyclical deformation was an integral part of vein development.

Robert & Kelly (1987) previously concluded that gold emplacement followed vein growth, because gold typically occurs in microcracks in common association with fluid inclusion planes. Because gold-bearing microcracks are truncated in some places by younger crack–seal increments, it is now believed that the gold was deposited episodically during the whole history of the veins.

Vein development and fluid dynamics

Repeated growth and deformation cycles during development of the subhorizontal extensional veins were clearly coupled with transient reversals in shortening direction that we ascribe to local stress variations. The fault-valve model proposed by Sibson *et al.* (1988) to explain such gold deposits also involves shear stress variations related to fluid pressure fluctuations and provides a framework for detailed analysis of the processes accompanying vein development.

High-angle, E–W reverse faults were unfavourably oriented for slip in the prevailing stress field responsible for the N–S shortening and could be reactivated only if fluid pressure exceeded lithostatic load and at low values of differential stress (Sibson 1985). High-angle reverse faults may then act as fluid-activated valves capping overpressured portions of the crust and promoting large cyclic fluctuations in fluid pressure, P_f (Fig. 15). As discussed by Sibson *et al.* (1988), seismic rupture along such faults is triggered by an increase in both P_f and shear stress along the fault. The vein systems are thus inferred to represent rupture nucleation sites within the fault zones. Before rupture, P_f reaches supralithostatic values, promoting the formation of the subhorizontal extensional veins. After shear failure, which releases shear stress along the fault, P_f decreases dramatically by fluid discharge through the extensive fracture permeability along the rupture zone. Pressure builds up again when the shear veins are re-sealed by mineral deposition.

In the light of our microstructural and fluid inclusion observations, the details of vein development are best discussed in a two-stage model in relation with the fault-valve model.

Stage 1: fluid pressure build up and opening of subhorizontal extensional veins. Incremental vertical opening of the subhorizontal extensional veins and open-space filling textures imply that fluid pressure was high enough to support the rock column above the vein, i.e. that fluid pressure was higher than the lithostatic load. The geometry of the subhorizontal veins with a vertical opening vector also indicates that these extensional fractures initiated by hydraulic fracturing under conditions of high fluid pressure,

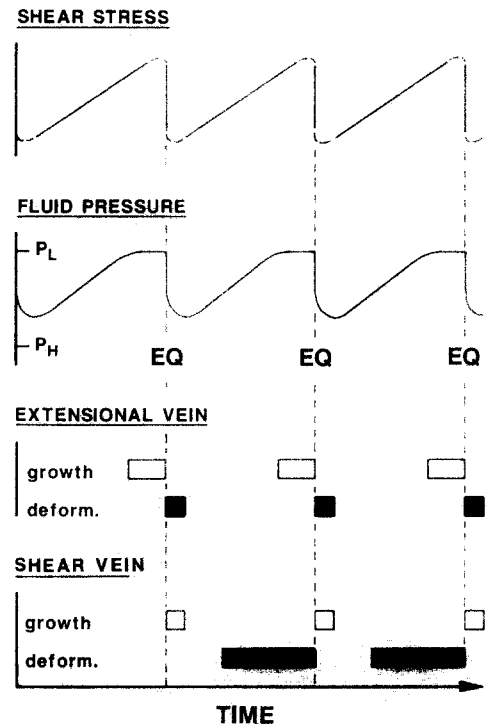

Fig. 15. Diagram showing shear stress variations and fluid pressure fluctuations with time, as predicted by the fault-valve model (Sibson *et al.* 1988); P_L, lithostatic pressure, P_H, hydrostatic pressure, EQ, earthquake. Growth and deformation stages of the extensional and shear veins are correlated with these variations.

$$P_f = \sigma_3 + T$$

and low differential stress,

$$\sigma_1 - \sigma_3 < 4T,$$

where T is the tensile strength of the rock (Secor 1965).

As crack–seal textures preserve the delicate geometry of the vein walls, it is suggested that these cracks propagated slowly, probably by subcritical crack growth. A crack may propagate slowly even if the stress concentration factor (K) at the tip of the crack is lower than the critical value K_c for catastrophic crack extension (Atkinson & Meredith 1987). The driving mechanism of subcritical crack growth could be stress corrosion at the crack tip enhanced by the presence of a fluid at supralithostatic pressure.

Subhorizontal fluid inclusion planes also correspond to very small opening increments of the subhorizontal extensional veins. They are different from the crack–seal structures in that they probably occur haphazardly across the width of the vein, as suggested by their greater number in the oldest growth layers than in the youngest. Their propagation mechanism is probably different from that of crack–seal planes because they are planar, sometimes branched, and cross-cut different minerals (quartz, tourmalines) or crack–seal lines. Consequently,

it is suggested that they result from fast crack growth ($K \geq K_c$).

The presence of clear quartz displaying Brazil twins between areas of tourmaline fibres, columnar inclusion-rich quartz, and crack–seal structures in subhorizontal extensional veins, suggests that those individual growth layers formed predominantly by crack–seal processes also contained local fluid-filled pockets during their formation. The existence of extensive fluid-filled cavities has been described as water-sills (Fyfe *et al.* 1978, Henderson *et al.* 1990) and may be very important in understanding some stages of the vein filling history.

The growth stages of the subhorizontal extensional veins reflect increase of fluid pressure (Fig. 15) and correspond to the pre-failure stage of the fault-valve model of Sibson *et al.* (1988). As subhorizontal extensional veins are connected with steeply dipping shear veins, their opening should correspond to a stage where the shear veins were sealed (permeability barrier). Corresponding textures in the shear veins above the seal point could be the observed stylolites (recording horizontal shortening of the veins) and plastically deformed quartz crystals. As fluid pressure builds up, crack–seal opening as well as development of microcracks (fluid inclusion planes) may also occur in the shear veins below the seal point.

If this correlation with the fault-valve model is correct, successive growth layers in subhorizontal extensional veins should have been separated in time by seismic rupture events along the neighbouring shear veins (Fig. 15).

Stage 2: *slip along shear veins, fluid pressure drop, and collapse of subhorizontal extensional veins.* Vertical shortening of the subhorizontal extensional veins took place episodically during vein formation. This deformation corresponds to collapse of the veins and is ascribed to a sudden drop in fluid pressure. It is not comparable in intensity to the deformation leading to the opening of the veins and is estimated to be around 1% or less of the whole thickness of a vein. Such transient and episodic drops in fluid pressure, alternating with episodes of high fluid pressure, are predicted by the fault valve model of Sibson *et al.* (1988) and are a consequence of post-rupture high fracture permeability along the fault zone. This stage of transient high permeability in shear veins is indicated by the observed open space filling textures.

The variety of quartz microstructures in shear veins can be explained by two alternating processes (see Drury & Urai 1990) and probably reflects both aseismic and seismic deformation along the fault zone. The first process involves dynamic recrystallization by rotation of subgrains leading to the formation of 50 μm grains and results from aseismic deformation. The second involves recrystallization by grain-boundary migration enhanced by shear stress drop and by the presence of a fluid phase, leading to the formation of larger (up to 400 μm) less deformed and clear quartz grains; this process is interpreted as the result of seismic rupture. These mechanisms may be cyclic or discontinuous in time (Drury & Urai 1990).

Evidence for local shear stress reversal

Microstructural and fluid inclusion observations presented above clearly indicate episodic vertical shortening during development of extensional veins. Such shortening is ascribed to sudden drop in P_f after rupture along neighbouring shear veins. This has important implications on local (vein scale) stress conditions: σ_1 must be vertical at the time of vertical shortening which in turn requires a total release of shear stress along adjacent shear veins after rupture.

The observed local normal faulting along shear veins (Fig. 10) is compatible with a total release of shear stress and may further indicate shear stress reversal. In addition, the formation of extensional veins by hydraulic fracturing implies that the differential stress was low (Secor 1965, Etheridge 1983), and that the level of shear stress along the fault prior to rupture must also have been relatively low. Under such conditions it is generally considered that there is an almost total release of shear stress after rupture along the fault (see Sibson 1989, p. 5). Given the low differential stress, it is conceivable that the total release of shear stress is accompanied by a transient reversal of stress axes, as suggested by the documented intermittent vertical shortening of the extensional veins.

Nature of the percolating fluids

Based on a fluid inclusion study of the Sigma deposit, Robert & Kelly (1987) interpreted the two dominant CO_2-rich and H_2O–NaCl fluids as resulting from unmixing of a parent H_2O–CO_2, low-salinity fluid due to pressure drops. It is now suggested that such pressure drops occurred at the time of seismic rupture along the shear veins.

One intriguing aspect of fluids revealed by the present study is the sample-scale partitioning of these two end-members fluids into microfractures of contrasting orientation in extensional veins (Figs. 12a and 14a). We propose that the physical separation of the two immiscible fluids is related to their very different wetting properties which become an important parameter in capillarity forces at small scale and high flow rates (Y. Gueguen written communication 1991). Recent experimental studies by Watson & Brenan (1987) have shown that the wetting or dihedral angle (θ) of a fluid in quartz at textural equilibrium decreases with increasing H_2O/CO_2 ratio and with increasing NaCl content. Thus, the CO_2-rich fluids have θ around 90° and the aqueous fluids may have θ as low as 40°. Assuming that the parent fluid infiltrates the extensional veins along subhorizontal microcracks, rupture along the shear vein induces P_f drop and fluid unmixing, as well as the formation of new vertical microcracks. Given their respective wetting properties, the CO_2-rich fluid would remain in the horizontal microcracks, and the H_2O–NaCl fluid would

be expelled in vertical microcracks. Such a phenomenon, similar to the 'wicking' process (Crawford & Hollister 1986), is locally observed at a small scale where short vertical aqueous fluid inclusion planes originate on longer horizontal CO_2-rich fluid inclusion planes.

It is not clear at present if this mechanism can explain fluid partitioning in shear veins. Given that these are drained systems connected with the reservoir and, intermittently, with higher crustal levels, additional factors may influence fluid distribution in microcracks, including escape of CO_2 along the fault (Parry & Bruhn 1990).

CONCLUSIONS

Subhorizontal extensional veins at Val d'Or are the result of successive vertical opening and collapse events, which may be related to episodes of sealing and seismic slip along adjacent shear veins, respectively. As proposed by Sibson *et al.* (1988), the opening of the extensional veins is due to hydraulic fracturing in a regional N–S compressional regime, in a lithostatic or supralithostatic fluid pressure environment. Structures such as crack–seal inclusion bands, fibres, stretched crystals and open-space filling crystals are attributed to hydraulic fracturing and probably subcritical crack growth. Primary fluid inclusions found in such structures and horizontal CO_2-rich fluid inclusion planes are related to the high fluid pressure episodes.

Episodic collapse of the subhorizontal veins is attributed to a dramatic fluid pressure drop related to seismic slip parallel to the shear veins. Vertical H_2O + NaCl fluid inclusion planes are characteristic of that low fluid pressure period and may indicate localized shear stress reversal post-failure.

The complex internal structures of the gold–quartz veins provide an excellent record of Archaean seismic activity along high-angle reverse faults. As shown by Parry & Bruhn (1990) for normal faults, fluid inclusion studies can provide evidence for, and quantify, fluid pressure fluctuations along faults. This study emphasizes the importance of fluid pressure in faulting and shows that combined microstructural and fluid inclusion studies of exhumed seismogenic faults may provide new insights in understanding earthquake processes along active faults.

Acknowledgements—We express our appreciation to R. H. Sibson, S. F. Cox, K. H. Poulsen, J. R. Henderson, M. N. Henderson and T. J. Reynolds for stimulating discussions and comments on various drafts of this paper, as well as to R. H. Sibson and R. L. Bruhn for their critical reviews. We also thank the staff and geologists of Sigma, New Pascalis and Dumont-Bras d'Or mines for their collaboration. This work was done while A.-M. Boullier was on sabbatical leave at the G.S.C., during which she benefited from a N.A.T.O. grant. She also thanks colleagues at the Mineral Deposits Division of the G.S.C. for their hospitality. Contribution C.R.P.G. No. 856, G.S.C. No. 54490, C.N.R.S.-I.N.S.U.-D.B.T. (thème Instabilités) No. 315.

REFERENCES

Atkinson, B. K. & Meredith, P. G. 1987. The theory of subcritical crack growth with applications to minerals and rocks. In: *Fracture Mechanics of Rocks* (edited by Atkinson, B. K.). Academic Press, London, 111–166.

Brace, W. F. & Bombolakis, E. G. 1963. A note on brittle crack growth in compression. *J. geophys. Res.* **68**, 3709–3713.

Brantley, S. L., Evans, B., Hickman, S. H. & Crerar, D. A. 1990. Healing of microcracks in quartz: implications for fluid flow. *Geology* **18**, 136–139.

Brown, P. E. & Lamb, W. M. 1986. Mixing of H_2O–CO_2 in fluid inclusions: geobarometry and Archean gold deposits. *Geochim. cosmochim. Acta* **50**, 847–852.

Cox, S. F. 1987. Antitaxial crack-seal vein microstructures and their relationship to displacement paths. *J. Struct. Geol.* **9**, 779–787.

Cox, S. F. & Etheridge, M. A. 1983. Crack-seal fibre growth mechanisms and their significance in the development of oriented layer silicate microstructures. *Tectonophysics* **92**, 147–170.

Cox, S. F., Etheridge, M. A. & Wall, V. J. 1986. The role of fluids in syntectonic mass transport, and the localization of metamorphic vein-type ore deposits. *Ore Geol. Rev.* **2**, 65–86.

Cox, S. F., Wall, V. J., Etheridge, M. A. & Potter, T. F. In press. Deformational and metamorphic processes in the formation of mesothermal vein-hosted gold deposits. Examples from the Lachlan fold belt in Central Victoria, Australia. *Ore Geol. Rev.*

Crawford, M. L. & Hollister, L. S. 1986. Metamorphic fluids: evidence from fluid inclusions. In: *Fluid–Rock Interaction During Metamorphism* (edited by Walther, J. V. & Wood, B. J.). Springer, New York, 1–35.

Dimroth, E., Imreh, L., Goulet, N. & Rocheleau, M. 1983. Evolution of the south-central segment of the Archaean Abitibi belt, Quebec. Part II: Tectonic evolution and geochemical model. *Can. J. Earth Sci.* **20**, 1355–1373.

Drury, M. R. & Urai, J. L. 1990. Deformation-related recrystallization processes. *Tectonophysics* **172**, 235–253.

Etheridge, M. A. 1983. Differential stress magnitudes during regional deformation and metamorphism: upper bound imposed by tensile fracturing. *Geology* **11**, 231–234.

Frondel, C. 1962. *The System of Mineralogy. Volume* III, *Silica Minerals*. John Wiley & Sons, New York.

Fyfe, W. S., Price, N. J. & Thompson, A. B. 1978. *Fluids in the Earth's Crust*. Elsevier, Amsterdam.

Gaumond, A. 1986. Le gite d'or de New Pascalis, Canton de Louvicourt, P.Q.: structure, minéralogie et altération associée aux veines. Unpublished M.Sc.A. thesis. Ecole Polytechnique, Montreal, Quebec.

Guha, J., Zu, H. Z., Dubé, B., Robert, F. & Gagnon, M. 1991. Fluid characteristics of vein and altered wallrock in Archean mesothermal gold deposits. *Econ. Geol.* **86**, 667–684.

Gunning, H. C. & Ambrose, J. W. 1937. Cadillac-Malartic area, Québec. *Trans. Can. Inst. Min. Metall.* **40**, 341–362.

Henderson, J. R., Henderson, M. N. & Wright, T. O. 1990. Water-sill hypothesis for the origin of certain veins in the Meguma Group, Nova Scotia, Canada. *Geology* **18**, 654–657.

Hubbert, M. K. & Rubey, W. W. 1959. Role of fluid pressure in the mechanics of overthrust faulting. Part I: Mechanics of fluid-filled porous solids and its application to overthrust faulting. *Bull. geol. Soc. Am.* **70**, 115–166.

Jemielita, R. A., Davis, D. W. & Krogh, T. E. 1990. U–Pb evidence for Abitibi gold mineralization postdating greenstone magmatism and metamorphism. *Nature* **346**, 831–834.

Kerrich, R. 1986. Fluid infiltration into fault zones: chemical, isotopic and mechanical effects. *Pure & Appl. Geophys.* **124**, 225–268.

Kerrich, R. 1989. Geodynamic setting and hydraulic regimes: shear zone hosted mesothermal gold deposits. In: *Mineralization and Shear Zones* (edited by Bursnall, J. T.). *Geol. Ass. Can., Short Course Notes* **6**, 89–128.

Kerrich, R. & Allison, I. 1978. Vein geometry and hydrostatics during Yellowknife mineralization. *Can. J. Earth Sci.* **15**, 1653–1660.

Krantz, R. L. 1979. Crack growth and development during creep of Barre granite. *Int. J. Rock Mech. & Mining Sci.* **16**, 23–35.

Krantz, R. L. 1983. Microcracks in rocks: a review. *Tectonophysics* **100**, 449–480.

Laubach, S. E. 1989. Paleostress directions from the preferred orientation of closed microfractures (fluid-inclusion planes) in sandstones, East Texas basin, U.S.A. *J. Struct. Geol.* **11**, 603–611.

Lespinasse, M. & Pêcher, A. 1986. Microfracturing and regional stress field: a study of the preferred orientations of fluid-inclusion planes in a granite from the Massif Central, France. *J. Struct. Geol.* **8**, 169–180.

Ludden, J., Hubert, C. & Gariepy, C. 1986. The tectonic evolution of the Abitibi greenstone belt of Canada. *Geol. Mag.* **123**, 153–166.

Parry, W. T. & Bruhn, R. L. 1990. Fluid pressure transients on seismogenic normal faults. *Tectonophysics* **179**, 335–344.

Phillips, W. J. 1972. Hydraulic fracturing and mineralization. *J. geol. Soc. Lond.* **128**, 337–359.

Ploegsma, M. 1989. Shear zones in the West Uusimaa area, SW Finland. Unpublished Ph.D. thesis, University of Amsterdam, The Netherlands.

Poulsen, K. H. & Robert, F. 1989. Shear zones and gold: practical examples from the southern Canadian Shield. In: *Mineralization and Shear Zones* (edited by Bursnall, J. T.). *Geol. Ass. Can., Short Course Notes* **6**, 239–266.

Ramsay, J. G. 1980. The crack–seal mechanism of rock deformation. *Nature* **284**, 135–139.

Ramsay, J. G. & Graham, R. H. 1970. Strain variations in shear belts. *Can. J. Earth Sci.* **7**, 786–813.

Ramsay, J. G. & Huber, M. I. 1983. *Modern Techniques of Structural Geology, Volume* 1: *Strain Analysis.* Academic Press, London.

Ren, X., Kowallis, B. J. & Best, M. G. 1989. Paleostress history of the Basin and Range Province in western Utah and eastern Nevada from healed microfracture orientations in granites. *Geology* **17**, 487–490.

Robert, F. 1989. The internal structure of the Cadillac tectonic zone southeast of Val d'Or, Abitibi belt, Quebec. *Can. J. Earth Sci.* **26**, 2661–2675.

Robert, F. 1990a. Structural setting and control of gold–quartz veins of the Val d'Or area, southeastern Abitibi Subprovince. In: *Gold and Base Metal Mineralization in the Abitibi Subprovince, Canada, With Emphasis on the Quebec Segment* (compiled by Ho, S. E., Robert, F. & Groves, D. I.). *Univ. West. Aust. Publ.* **24**, 164–209.

Robert, F. 1990b. An overview of gold deposits in the Eastern Abitibi belt. In: *The Northwestern Quebec Polymetallic Belt* (edited by Rive, M., Verpaest, P., Gagnon, Y., Lulin, J. M., Riverin, G. & Simard, A.). *Can. Inst. Min. Metall.* **43**, 93–105.

Robert, F. & Brown, A. C. 1986a. Archaean gold-bearing quartz veins at the Sigma mine, Abitibi greenstone belt, Quebec. Part I: Geologic relations and formation of the vein system. *Econ. Geol.* **81**, 578–592.

Robert, F. & Brown, A. C. 1986b. Archaean gold-bearing quartz veins at the Sigma mine, Abitibi greenstone belt, Quebec. Part II: Vein paragenesis and hydrothermal alteration. *Econ. Geol.* **81**, 593–616.

Robert, F., Brown, A. C. & Audet, A. J. 1983. Structural control of gold mineralization at the Sigma Mine, Val d'Or, Quebec. *Bull. Can. Inst. Min. Metall.* **76**, 72–80.

Robert, F. & Kelly, W. C. 1987. Ore-forming fluids in Archaean gold-bearing quartz veins at the Sigma Mine, Abitibi greenstone belt, Quebec, Canada. *Econ. Geol.* **82**, 1464–1482.

Roedder, E. 1984. Fluid inclusions. *Miner. Soc. Am. Rev. Miner.* **12**.

Secor, D. T. 1965. Role of fluid pressure in jointing. *Am. J. Sci.* **263**, 633–646.

Sibson, R. H. 1981. Controls on low-stress hydro-fracture dilatancy in thrust, wrench and normal fault terrains. *Nature* **289**, 665–667.

Sibson, R. H. 1985. A note on fault reactivation. *J. Struct. Geol.* **7**, 751–754.

Sibson, R. H. 1989. Earthquake faulting as a structural process. *J. Struct. Geol.* **11**, 1–14.

Sibson, R. H. 1990. Faulting and fluid flow. In: *Fluids in Tectonically Active Regimes of the Continental Crust* (edited by Nesbitt, B. E.). *Miner. Ass. Can., Short Course Handbook* **18**, 93–132.

Sibson, R. H., Robert, F. & Poulsen, K. H. 1988. High angle reverse faults, fluid-pressure cycling, and mesothermal gold–quartz deposits. *Geology* **16**, 551–555.

Smith, D. L. & Evans, B. 1984. Diffusional crack healing in quartz. *J. geophys. Res.* **89**, 4125–4135.

Tapponnier, P. & Brace, W. P. 1976. Stress induced microcracks in Westerly granite. *Int. J. Rock Mech. & Mining Sci.* **13**, 103–112.

Tessier, A. C. 1990. Structural evolution and host rock dilation during emplacement of gold–quartz veins at the Perron deposit, Val d'Or, Quebec. Unpublished M.Sc. thesis, Queens University, Kingston, Ontario.

Tuttle, O. F. 1949. Structural petrology of planes of liquid inclusions. *J. Geol.* **57**, 331–356.

Vu, L. 1990. Geology of the Ferderber gold deposit and potential of the Bourlamaque batholith, Belmoral Mines Ltd., Quebec. In: *The Northwestern Quebec Polymetallic Belt* (edited by Rive, M., Verpaest, P., Gagnon, Y., Lulin, J. M., Riverin, G. & Simard, A.). *Can. Inst. Min. Metall.* **43**, 255–268.

Watson, E. B. & Brenan, J. M. 1987. Fluids in the lithosphere. 1. Experimentally determined wetting characteristics of CO_2–H_2O fluids and their implications for fluid transport, host-rock physical properties and fluid inclusion formation. *Earth Planet. Sci. Lett.* **85**, 497–515.

Wise, D. U. 1964. Microjointing in basement, middle Rocky mountains of Montana and Wyoming. *Bull. geol. Soc. Am.* **75**, 287–306.

Wong, L., Davis, D. W., Hanes, J. A., Archibald, D. A., Hodgson, C. J. & Robert F. 1989. An integrated U/Pb and Ar/Ar geochronological study of the Archaean Sigma gold deposit, Val d'Or, Quebec. *Geol. Ass. Can., Miner. Ass. Can., Joint Annual Meeting, Prog. w. Abs.* **14**, A45.

Zweng, P. L. & Mortensen, J. K. 1989. U/Pb age constraints on Archaean magmatism and gold mineralization at the Camflo mine, Malartic, Quebec. *Geol. Soc. Am., Annual Meeting, Abs. w. Prog.* **A351**.